Front. Earth Sci. 2021, 15(2): 343–359
https://doi.org/10.1007/s11707-021-0913-x

RESEARCH ARTICLE

Differences in shale gas accumulation process and its significance in exploration of Lower Silurian Longmaxi Formation in northeast Yunnan

Shangbin CHEN (✉)[1,2], Huijun WANG[2], Yang WANG[1,2], Tianguo JIANG[3], Yingkun ZHANG[2], Zhuo GONG[2]

1 Key Laboratory of Coalbed Methane Resources and Reservoir Formation Process of the Ministry of Education, China University of Mining and Technology, Xuzhou 221116, China
2 School of Resources and Geoscience, China University of Mining and Technology, Xuzhou 221116, China
3 Yunnan Coalbed Methane Resources Exploration and Development Co., Ltd, Kunming 650031, China

Abstract The study and exploration practice of shale gas accumulation has focused on the static system comparison, key parameters analysis, reservoir characteristics, enrichment mode etc. However, the research on dynamic recovery from the original hydrocarbon generation of shale gas to the present gas reservoir is still lacking. The burial history of shale gas reservoir can reflect the overall dynamic process of early formation and later transformation of shale gas reservoir. It controls the material basis of shale gas, the quality of reservoir physical properties, preservation conditions, gas content and formation energy, which is the core and foundation of shale gas accumulation process research. Herein, based on the five typical wells data in the Northeast Yunnan, including geochronological data, measured R_o values, core description records, well temperature data, paleoenvironment, paleothermal, etc., the burial history, thermal evolution history and hydrocarbon generation history of the Lower Silurian Longmaxi Formation were systematically restored via back stripping method and EASY%R_o model. The results show that 1) the differences in the burial history of marine shale in Longmaxi Formation can be divided into syncline type and anticline type. 2) The shale gas accumulation process can be divided into four stages, namely the source-reservoir-cap sedimentation period, initial accumulation period, main accumulation period, and adjustment period. 3) Based on the characteristics of burial history and preservation conditions, the areas with wide and gentle anticline, far away from the denudation area, and buried deeply with good fault sealing ability are priority structural locations for the shale gas exploration in northeast Yunnan.

Received February 25, 2021; accepted May 12, 2021

E-mail: shangbinchen@163.com

Keywords shale gas, accumulation process, exploration significance, Longmaxi Formation (Fm.), northeast Yunnan

1 Introduction

The shale gas reservoir formation is closely related to the shale thickness, burial depth, organic carbon content, and organic matter maturity (Zhang et al., 2019; Yang et al., 2020). The burial history, thermal evolution history, and hydrocarbon generation history (hereinafter referred to as "three history") of source rocks control the hydrocarbon generation process of shale gas by changing the sedimentation-diagenesis, burial depth, and thermal evolution of the formation via tectonic movement; thus, affect the shale gas accumulation process (Luo and Vasseur, 1992; Wu et al., 1993; Luo, 1998; Zhu et al., 2014; English et al., 2016; Chen et al., 2017a; Gottardi et al., 2019; Pang et al., 2020; Zhang et al., 2020a). The macroscopic fracture fold structure and microscopic pore and fracture system formed by the late tectonic deformations affect the reservoir characteristics, enrichment mode, and migration methods of the shale gas. Therefore, apart from being related to the early construction process of the shale gas accumulation, the "three history" also has a profound impact on the later transformation process.

The study area, namely Northeastern Yunnan, is located in the upper Yangtze region. In the long geological history, it has experienced several periods of tectonic movements with different properties, which had a great impact on the generation, migration, and preservation of oil and gas (Yuan et al., 2010; Cao et al., 2018; Feng et al., 2019). The sedimentary history and tectonic history of the Sichuan Basin have been reported by the analysis of denudation at any point on the profile (Liu and Chang, 2003; He et al.,

2020). Yang et al. (2020) calculated the paleoproductivity and major limiting factors of Longmaxi Formation (Fm.) through the zircon U-Pb dating, principal trace elements, and spectral analysis (Yang et al., 2020). By verifying the burial history data, Zhang et al. (2019) concluded that the drilling depth for good shale gas production capacity should be at least 1019–1529 m. By the restoration of burial history, Wo et al. (2007a) divided the multi-phase subsidence and uplift of the marine strata in southern China since the Indosinian movement into two major types and six types of burial, namely "early subsidence and late uplift" and "early uplift and late subsidence". Yuan et al. (2010) reconstructed the burial history of the middle and upper Yangtze region by the back-stripping method, and divided it into three main types: the early uplift sustained type, the early uplift and then descend type, and the late uplift persistent type. Northeast Yunnan is located on the south-west edge of the Sichuan Basin. There are great variations in the tectonic evolution and less attention has been paid toward the difference in hydrocarbon accumulation process in different structural positions. Therefore, herein, based on the data of geochronology, R_o measured values, drilling core description records, logging curves, well temperature measured data, paleoenvironment, and paleotemperature data, the "three history" of Longmaxi Fm. shale in northeast Yunnan was reconstructed via the basin simulation technology. Also, the differences in "three history" evolution and accumulation process of different structural units were compared. The favorable structural positions of shale gas enrichment were selected with regards to the accumulation process and preservation, which can provide guidance for the efficient exploration of shale gas in this area.

2 Geological framework

The study area is located in the northern part of the Dianqianbei sag, the southwest margin of the Sichuan Basin, and the eastern edge of the Kangdian uplift. The area exists in the Leibo syncline and Daguan-Junlian anticline in the first-level structural unit of the Dianqianbei sag (Fig. 1). The tectonic features in the area are mainly NE, NW, and nearly NS directions, the folds are primarily composed of micro-trough type, and the faults are mainly thrust and strike-slip (Chen and Xiao, 1992; Yang et al., 2010; Qin et al., 2020). The structure of the area is complex, anticline area is strongly eroded, faults are intensively developed, and strata are integral. From the bottom to top, the strata are Upper Proterozoic Sinian, Paleozoic Cambrian, Ordovician, Silurian, Devonian, Carboniferous, Permian, Mesozoic Triassic, Jurassic, and Cretaceous. The Paleozoic marine strata and Meso Cenozoic continental strata are widely distributed. However, due to the influence of late structure, some strata suffered different degrees of denudation; therefore, Devonian, Carboniferous, Triassic, Jurassic, and Lower Cretaceous strata were all denuded. Taking Huayinshan Fault as the boundary, and a total of five wells with the most complete information were selected on the northwest

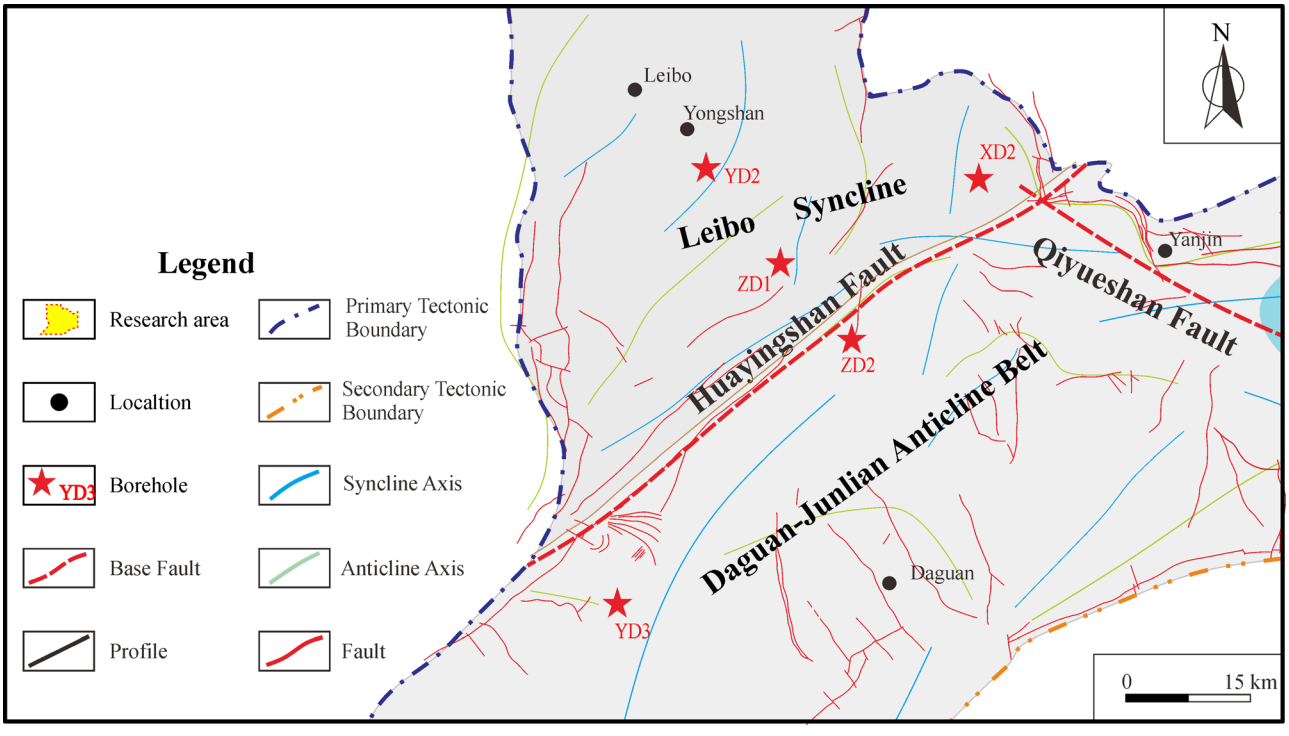

Fig. 1 Study area location and structure outline map.

and southeast sides, namely the, YD2, ZD1, XD2, ZD2, and YD3 wells.

3 Methods and modeling parameters

3.1 Basic simulation method

Herein, we used the basin simulation software PetroMod 2012 and paleo-heat method. The average temperature of paleo-surface was 24°C. The EASY%R_o model proposed by Sweeney and Burnhan was employed for the thermal evolution model of organic matter (Sweeney and Burnham, 1990). The measured vitrinite reflectance was taken as the calibration value, and the denudation amount and paleogeothermal gradient of each period were coupled to restore the burial history. The thermal maturity (i.e., vitrinite reflectance) was consistent with the measured value in order to recover the thermal evolution history and hydrocarbon generation history. The simulation process was consistent with the reported works (Waples, 1980; Burnham and Sweeney, 1989; Sweeney and Burnham, 1990; Morrow and Issler, 1993; Chen et al., 2017b). Herein, the compaction model was used to restore the geological history. The back stripping method was selected, i.e., starting from the present situation of the study area, the original sedimentary thickness of each stratum in different geological history stage was deduced in order to restore the original appearance of the stratum.

Using this model to restore the subsidence history of the formation is essential to restore porosity evolution in the formation. Therefore, the ancient thickness could be restored by using the relationship between the porosity and depth. It is assumed that the lateral position of the stratum remained unchanged in the process of subsidence and only the longitudinal position was changed. Therefore, the decrease in formation volume can be considered as the decrease in formation thickness. Under normal compaction, the relationship between the porosity and depth follows an exponential distribution as follows (Qiu et al., 2015; Zhang et al., 2016):

$$\Phi = \Phi_0 e^{-cz}, \tag{1}$$

where Φ is the porosity at depth z, %; Φ_0 is the surface porosity, %; c is the compaction coefficient, and z is the depth corresponding to porosity Φ. Using surface porosity Φ_0, arbitrary depth z, and its corresponding porosity Φ, the compaction constant c at the well was calculated.

The thickness of the rock skeleton was obtained by using the compaction constant and the depth of top and bottom boundary of each layer was calculated as follows:

$$H_s = (z_2 - z_1) - \frac{\Phi_0}{c}[e^{-cz_1} - e^{-cz_2}], \tag{2}$$

where H_s is the thickness of the rock skeleton, and z_1 and z_2 are the depth of the current top and bottom boundary of each layer, respectively.

$$z_2 = (H_s + z_1) + \frac{\Phi_0}{c}[e^{-cz_1} - e^{-cz_2}]. \tag{3}$$

Using the above steps, the skeleton thickness was calculated according to the current thickness of each stratum. Then, layer by layer was stripped back according to the sequence of the geological age from the latest to earliest, and the thickness of each stratum was recalculated for the each stripping layer. Finally, the thickness of each stratum in each geological period was calculated in order to complete the burial history restoration.

3.2 Selection of main parameters

3.2.1 Stratum

The study area is located in the southwestern margin of the Sichuan Basin, and the main body belongs to the Emei stratigraphic division of the Upper Yangtze stratigraphic division with well-developed strata. The Paleozoic marine and Mesozoic Cenozoic continental strata are widely distributed, but due to the impact of the late structure, some strata suffered different degrees of denudation in a few areas. In combination with previous research (Xu, 1981; Ye et al., 1983; Fang, 2000; Zhou et al., 2018), this article considered that the lack of Devonian and Carboniferous strata in the study was not due to the sedimentary interruptions, but to the denudation after deposition. There were two denudation processes in the area. The first occurred at 350–250 Ma, which denuded the Devonian and Carboniferous strata with maximum denudation amount of about 1300 m. The second occurred around 130 Ma, which eroded the Triassic, Jurassic, and Cretaceous strata with the erosion thickness of more than 4000 m.

3.2.2 Paleo-heat flow

The terrestrial heat flow in the research area was investigated (Yuan et al., 2006; Lu et al., 2007; Liu, 2008; Wang et al., 2011; Straka and Sýkorová, 2018; Zamansani et al., 2019). The results show that although there were clear differences in the paleogeothermal flow and its variation (manifested in the peak value of geothermal flow, ascending and descending rate of terrestrial heat flow value, and duration of high value of terrestrial heat flow), there was a common change trend. In other words, since the Late Paleozoic, the terrestrial heat flow value of the area changed from low to high, and then, lowered again. From the early Paleozoic to early Permian, the northeast of Yunnan displayed the characteristics of low geothermal field, corresponding to the geothermal value of about 60 W/m^2. Xiaojiang fault zone, adjacent to

the research area, is the eruption channel of the Emeishan basalt. During the eruption period, the heat flow response of the study area was relatively strong (Fig. 2, Table 1), and the geothermal flow value may have exceeded 85 W/m^2. After Permian, the terrestrial heat flow value decreased gradually, but it was still at a relatively high level compared with that before Permian.

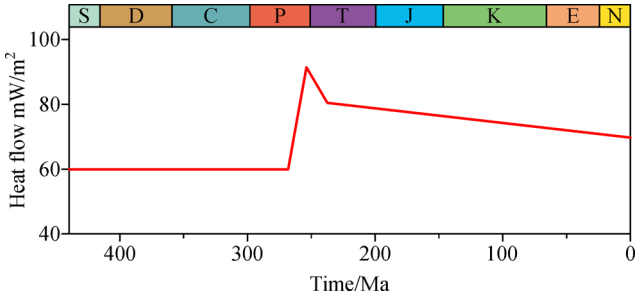

Fig. 2 Terrestrial heat flow value of research area (Jiang, 2016).

3.2.3 Paleo-environment

Paleobathymetry can be estimated via sedimentary facies analysis and paleontological assemblage data (Luo et al., 2017; Nie et al., 2020; Zhang et al., 2020b). Some elements are closely related to the environmental evolution of the hydrocarbon source rocks and are widely used for the paleo-water depth restoration. For instance, the ratio m of the main element MgO to Al_2O_3 and the correlation between CaO and Fe can be used as the indicators of salinity in the environment where the sediment was formed (Jiang, 1994). The value of m less than 1 signifies the freshwater sedimentary environment. The transition facies of sea-continent sedimentary environment is $1 \leqslant m < 10$, while the marine sedimentary environment is $10 < m < 100$. CaO/(Fe + CaO) < 0.2 denotes low salinity, 0.2–0.5 is medium salinity, and greater than 0.5 denotes high salinity (Jiang, 1994; Zhao and Yan, 1994; Teng et al., 2004). The m value of siliceous rock series in Longmaxi Fm. ranged from 4.96 to 36.88 with 11.75 as average, and the CaO/(Fe + CaO) value ranged from 0.017 to 0.831 with 0.29 as average. The results indicate that the salinity of the seawater in the study area during the deposition period was low, and it was a medium-low salinity seawater environment (Zhang et al., 2017). The paleo-water depth value during the deposition of Longmaxi Fm. in the Middle-Upper Yangtze region has not reached a consensus. Some paleontologists believe that the black graptolite shale and siliceous shale were formed at the depth of 30–100 m (Xiao et al., 1996; Qiu et al., 2018), while most sedimentary geologists believe that the black organic-rich shale was formed in the deep-water shelf (Bai et al., 2019; Pu et al., 2020) (according to the marine deposition model, the water depth should be 50–200 m). In the early deposition stage of Longmaxi Fm., a large-scale transgression occurred due to rapid melting of ice sheet. The Longmaxi Fm. in the study area was deposited in the deep-water shelf sedimentary environment. Several underwater uplift zones appeared locally due to the intensification of tectonic movements. These underwater uplift zones played the role of a barrier to a certain extent, and forming a limited stagnant sedimentary environment characterized by the deposition of a set of black carbonaceous shale. During the deposition of the Lower Silurian Longmaxi Fm., the

Table 1 Boundary conditions of terrestrial heat flow and ancient water depth

Boundary condition	Time/Ma	Well name				
		XD2	ZD1	ZD2	YD2	YD3
Ancient water depth/m	437	100	117	89	50	44
	426	95	113	86	49	44
	422	95	113	86	49	44
	352	77	88	71	45	42
	270	56	61	53	43	41
	134	27	27	27	27	27
	16	4	4	4	4	4
Terrestrial heat flow/(mW·m^{-2})	450	52	62	62	62	62
	439	44	54	54	54	54
	360	45	55	55	55	55
	290	65	85	80	100	100
	260	69	100	110	108	114
	240	63	92	90	100	105
	130	59.3	82	63	79	83
	0	55	63.1	63.1	70	63.1

water body often formed a "double-layer water" structure, which is conducive for the generation and preservation of organic matter. The black carbonaceous shale deposited in this period are an important set of high-quality source rocks in the Yangtze area. Thereafter, with the gradual decrease in sea level, the deep sea water mixed with the surface seawater for a long duration, which destroyed the anoxic environment at the bottom and deteriorated the preservation conditions of the organic matter. Simultaneously, the supply of terrigenous clasts relatively increased, causing a gradual decrease in the organic carbon content of Longmaxi Fm. from bottom to top. Herein, in combination with sedimentary facies, m value and the relationship between CaO and Fe and paleobathymetry of Longmaxi Fm. were determined (Fig. 3). The main body was located at 20–150 m.

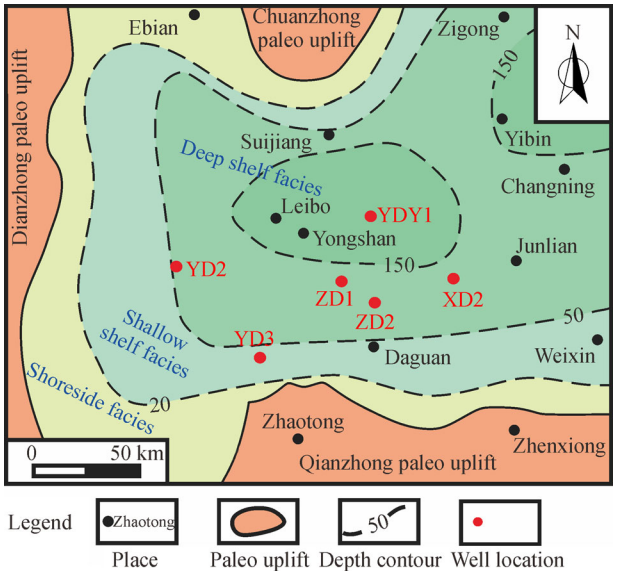

Fig. 3 Sedimentary facies and paleobathymetry of early Silurian Longmaxi Fm. (Modified from Bai et al. (2019)).

4 Results

4.1 Burial history

The simulation results of burial history show that the study area experienced multiple tectonic evolution events since the Cambrian deposition (Fig. 4), including the Caledonian, Hercynian, Indosinian, Yanshanian, and Himalayan movements, presenting a continuous traceable regional unconformity. The Devonian and Carboniferous strata were denuded under the influence of Hercynian movement. From Triassic to Cretaceous, they were completely denuded under the impact of Yanshanian movement and Himalayan orogeny. During the Caledonian and Hercynian movements, the strata were buried up to 2000 m, with the deepest one being nearly 3000 m. Afterwards, owing to the Yunnan Movement and the Dongwu Movement in the late Hercynian Movement, the uplifting and denudation happened, completely denuding the Devonian and Carboniferous strata. During the early stage of the Indosinian movement, the Emei tafrogeny movement and magmatic activity widely covered the area with basalt. Later, under the joint control of the Indosinian and Yanshanian movement, the stratum continued to be buried. The stratum reached its maximum burial depth of more than 6500 m at the beginning of the Early Cretaceous. Since then, the Indian plate continued to squeeze northwards, and the Eastern Pacific plate subducted westwards. Under the combined action of these two sets of compressive stresses, the upper Yangtze region continued to rise, resulting in the complete denudation of Triassic, Cretaceous, and Jurassic systems. Therefore, most of the drilling strata in the area are Permian, which directly cover the Silurian or Devonian system.

4.2 Thermal evolution history

Based on the shale maturity parameters, the simulation results were calibrated with the measured data and were in good agreement with the measured data, which verifies the reliability of the model and simulation results (Fig. 5). As per the maturity evolution curve, the period from Triassic to Cretaceous was the period with largest maturity variation range. During this period, the depth of the formation increased sharply, ground temperature rose rapidly (Fig. 6), and maturity also amplified accordingly. The measured data demonstrates that the maturity of the Longmaxi Fm. reached up to 3.5% (Fig. 5). The results of the geothermal simulations show that the temperature of Longmaxi Fm. had an overall upward trend before Permian (Fig. 6). Based on the analysis of regional and research area burial history, there were significant geothermal anomalies around the Permian because of the Emei tafrogeny and magmatic activity. The rate of geothermal rise in the early Triassic accelerated and reached maximum in the early Cretaceous strata. According to the simulation results of the maturity evolution (Fig. 5), the paleogeothermal and maturity evolution of the Longmaxi Fm. in the study area were controlled by the multi-stage tectonics and thermal activities. Also, the maturity evolution of organic matter could be divided into three stages. In the first stage (late Caledonian and Hercynian), the maturity of organic matter was in general not high, and most of it had not entered the low-maturity stage. In the second stage, Indosinian and Yanshanian, with an increase in the burial depth, the maturity increased and entered the stage of high maturity or over maturity, respectively. In the third stage (late Yanshanian and Himalayan), the stratum began to rise and maturity did not increase.

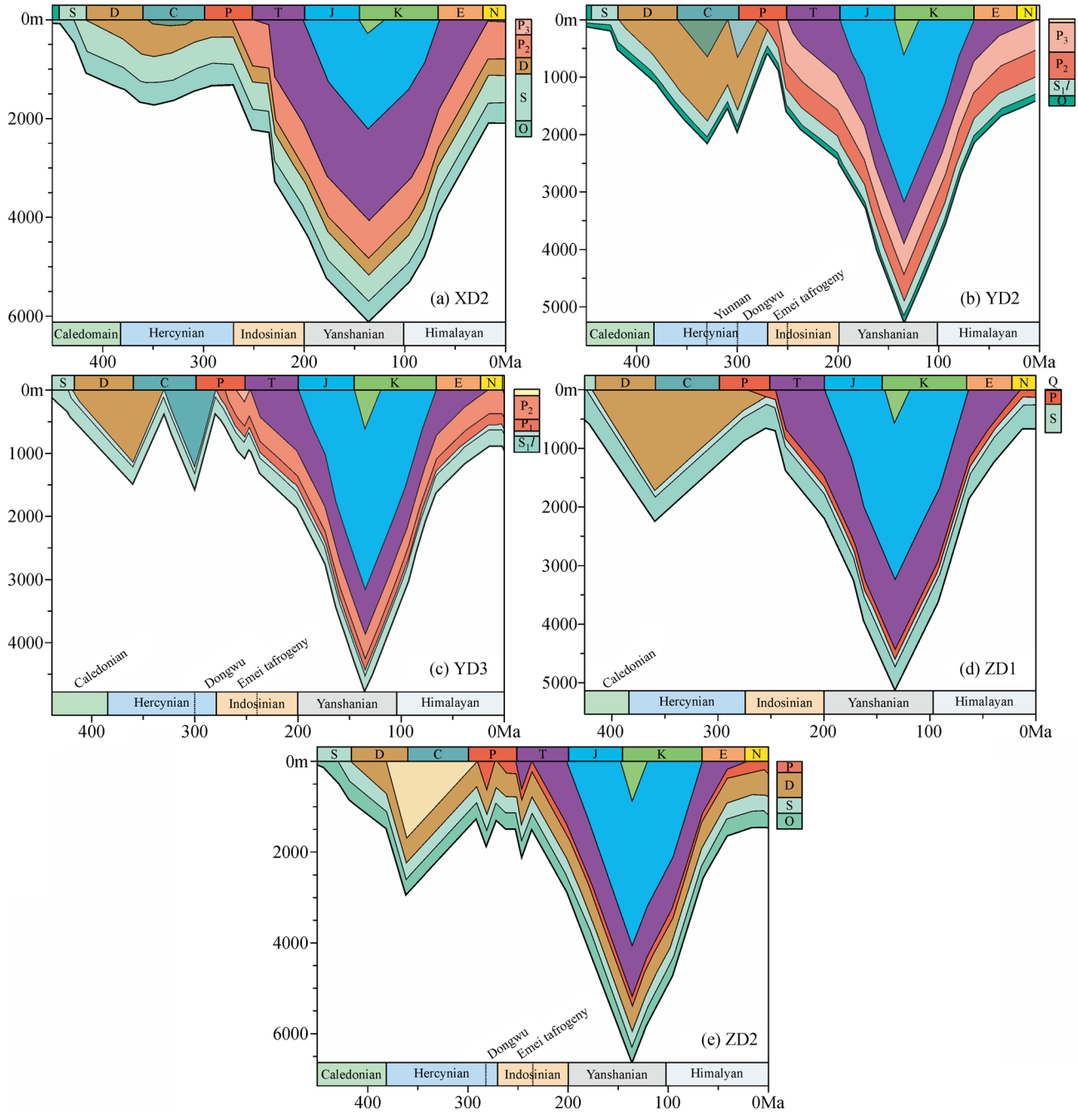

Fig. 4 Five typical well simulation results of burial history of (a) XD2; (b) YD2; (c) YD3; (d) ZD1; (e) ZD2.

4.3 Hydrocarbon generation history

Comparing the results of hydrocarbon generation history of each well, the hydrocarbon generation history of each well in the study area is both consistent and different (Fig. 7). The consistency was present in the hydrocarbon generation stage, i.e., R_o reached 0.7% in the early and middle Triassic, entering the middle mature oil generation stage. R_o reached 1.3% in the late Triassic, entering the high mature gas generation stage, while R_o reached 2.0% in the early middle Jurassic, entering the peak stage of mature gas generation. The thermal evolution was finalized in the early Cretaceous, and R_o no longer increased. The difference is manifested in the time of each well entering the hydrocarbon generation threshold. R_o of YD2 well, YD3 well, and ZD1 well reached 0.5% in the late Carboniferous strata, R_o of XD2 well reached 0.5% in the middle Permian strata, and R_o of ZD2 well reached 0.5% in the late Devonian strata. Owing to different structural locations and burial depth of each wells during

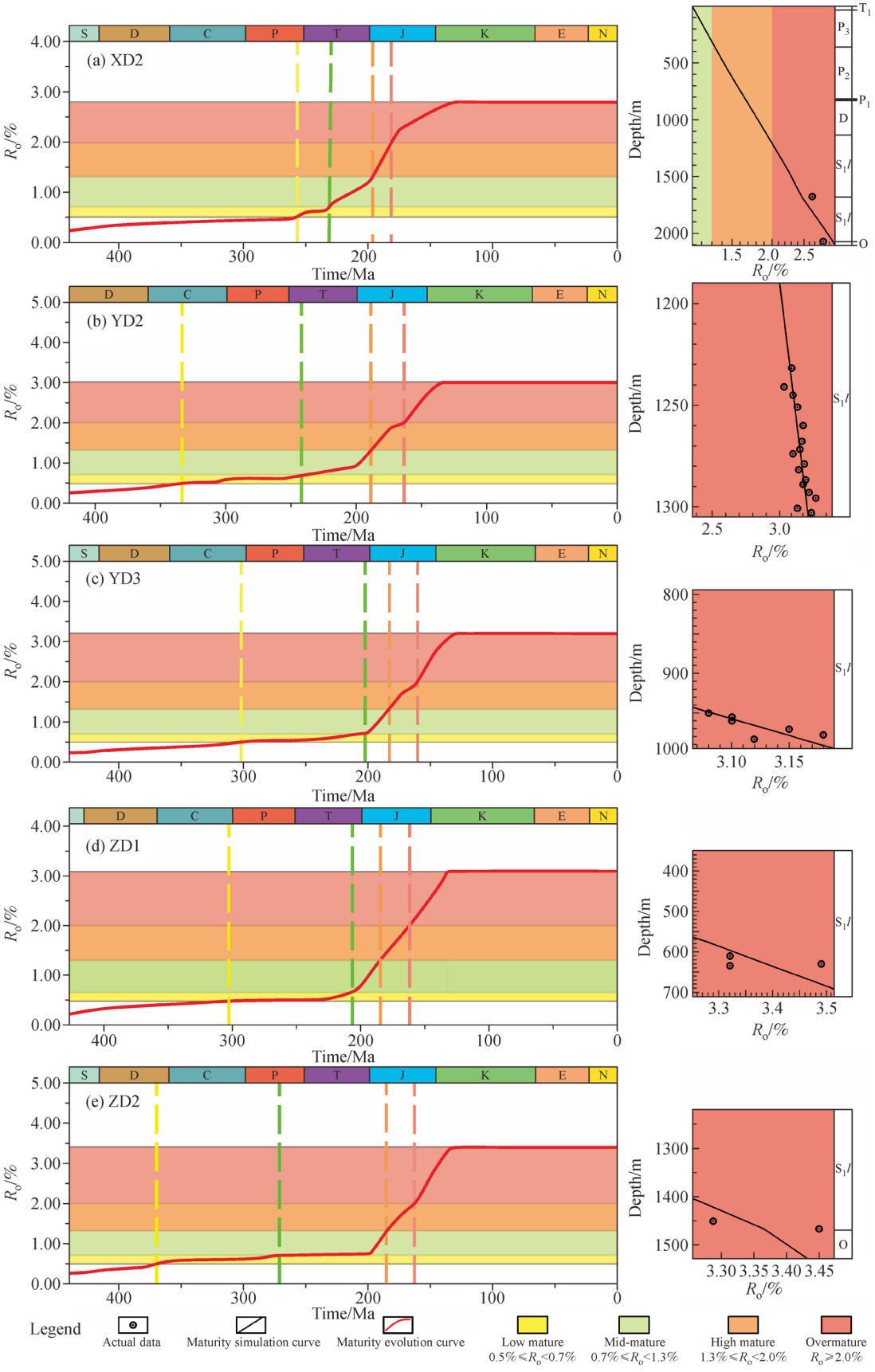

Fig. 5 Maturity evolution simulation curve and maturity calibration map of Longmaxi Fm. of (a) XD2; (b) YD2; (c) YD3; (d) ZD1; (e) ZD2.

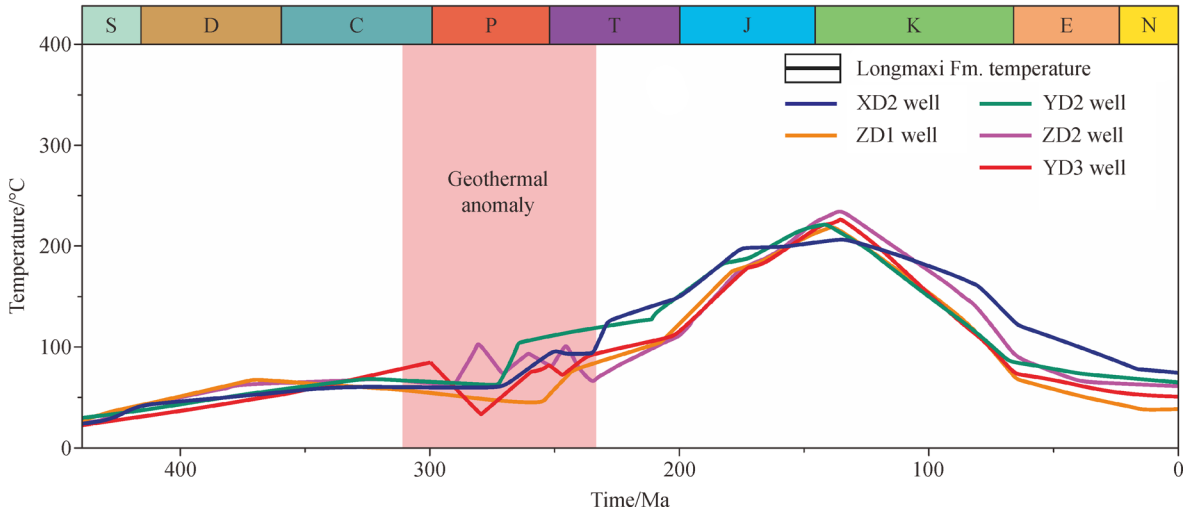

Fig. 6 Geothermal evolution curve of Longmaxi Fm.

the first burial process, XD2 well displayed shallowest burial depth and entered the hydrocarbon generation threshold later. While ZD2 well had a large burial depth and entered the hydrocarbon generation threshold at the earliest. Also, the thermal evolution of YD2, YD3, ZD1, and ZD2 wells during the hydrocarbon generation and oil generation process (R_o was between 0.5%–0.7%) was slow and long-term. One possible reason for the phenomenon is that at the beginning of the hydrocarbon generation stage of these wells, the formation began to rise slowly and the temperature and pressure of the formation gradually decreased. Therefore, the organic matter hydrocarbon generation conditions could not continue to be met, resulting in a slower maturity evolution, or even, stagnation. Later, in the second burial process, the depth of the stratum increased, the temperature of the stratum raised, and the organic matter displayed secondary hydrocarbon generation.

5 Discussion

5.1 Reservoir thickness characteristics

The sedimentary sequence of the Longmaxi Fm. in the research area transitioned from the middle and lower part of the carbonaceous shale and silty carbonaceous shale to the upper silty mudstone. There were numerous graptolite fossils and bioclasts in the middle and lower parts of the shale. There were more limestone lenses in the bedding direction of the shale and pyrite nodules were found locally. The stratum changed to light gray, grayish green, and grayish yellow from the bottom to the top with a small amount of calcareous. The top part could be distinguished from Huanggexi Fm. by gray medium thick limestone outcrop. The Longmaxi Fm. displayed a gradual thickening trend from the southwest to northeast (Fig. 8). The dark blue part in the figure is the high-quality shale section of Longmaxi Fm. with TOC > 2% and the thickness of 59–120 m in EW section (Fig. 8(a)) and 27–78 m in NS section (Fig. 8(b)). The burial depth of Longmaxi Fm. in the area was generally between 1000 m and 2500 m. The southern part was relatively shallow with a maximum depth of 2000 m, while the northern part was relatively deep with a maximum depth of 3500 m. The thickness and burial depth of source rocks played a vital role in controlling the hydrocarbon generation and shale gas preservation. The burial depth of Longmaxi Fm. was variable due to complex tectonic background in the area. Determining the burial depth conditions suitable for preservation is a useful index to evaluate the current preservation conditions of gas reservoirs.

5.2 Classification of regional burial history

Several regional tectonic movements occurred in the southern China, including Caledonian and Hercynian movement during the construction period of marine sedimentary basin (Sinian to Triassic), and Indosinian movement, Yanshanian movement, and Himalayan movement in the continental basin construction and marine basin reconstruction stage (Triassic to Quaternary) (Fig. 4). The different forms and intensities of tectonic movements in different areas led to different types of burial history of sedimentary strata in different structural parts (Gao et al., 2001; Wo et al., 2006, 2007a; Xiao et al., 2006). The uplift, deposition, and denudation because of varied tectonic movements in different regions were clearly dissimilar, resulting in different hydrocarbon generation evolution. According to whether the hydrocarbon generation process was continuous and if the mature evolution had reached or exceeded the peak period of hydrocarbon generation

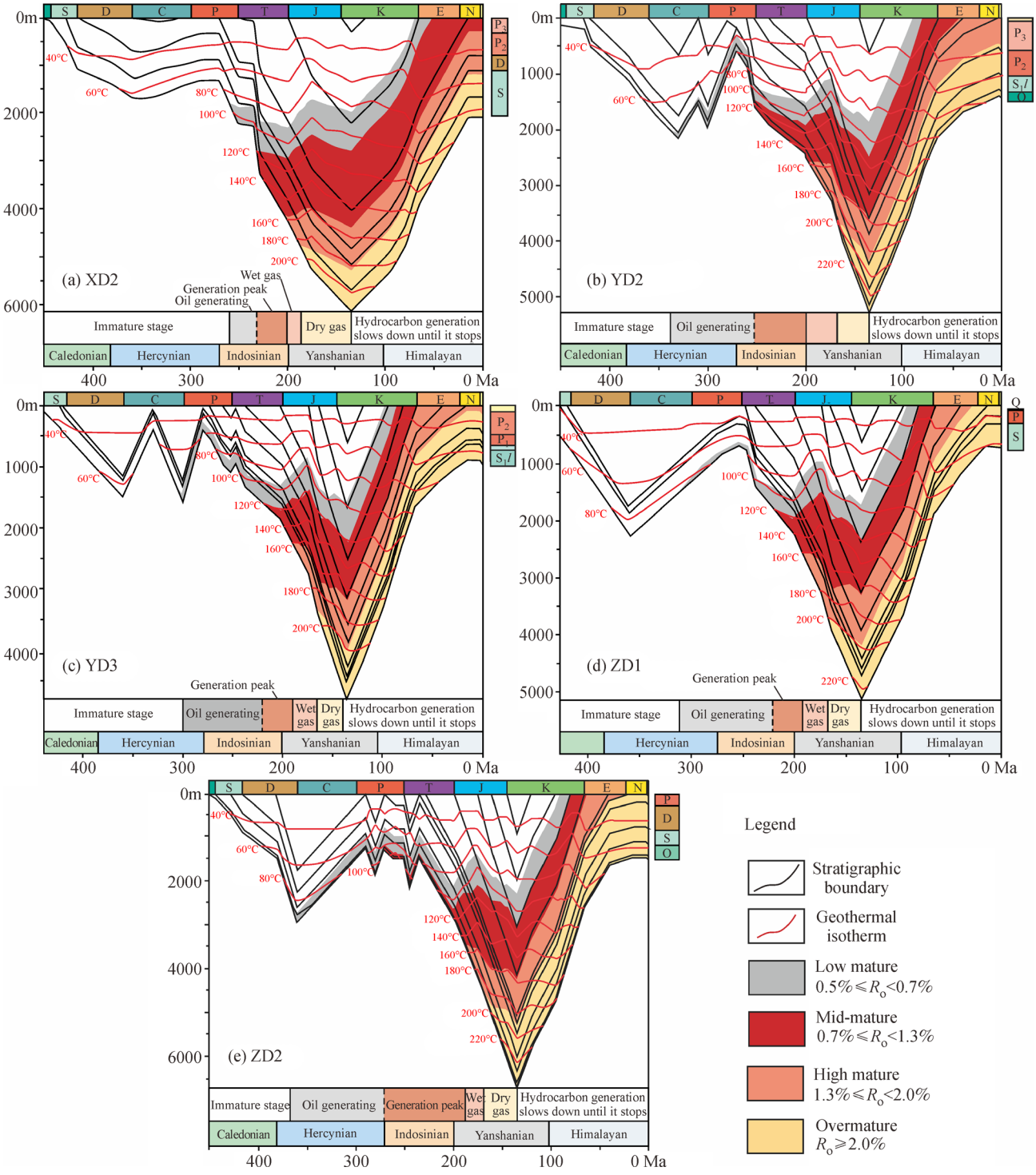

Fig. 7 Simulation results of hydrocarbon generation history and division of hydrocarbon generation stages. First line at the bottom of figure is division of hydrocarbon generation stages and second line is period of tectonic movement.

before the clear pause, the predecessors classified the burial history of the southern marine strata into "early subsidence, late uplift" and "early uplift, late subsidence" types (Wo et al., 2006, 2007b; Xiao et al., 2006; Yuan et al., 2010). The "early subsidence and late uplift" type included Sichuan type and Dianqiangui type (Fig. 9). The similarities between the Sichuan and Dianqiangui type lie in the early subsidence and late uplift, while the differences exist in that the subsidence period of the Sichuan type was long and the uplift period was short, and the accumulation

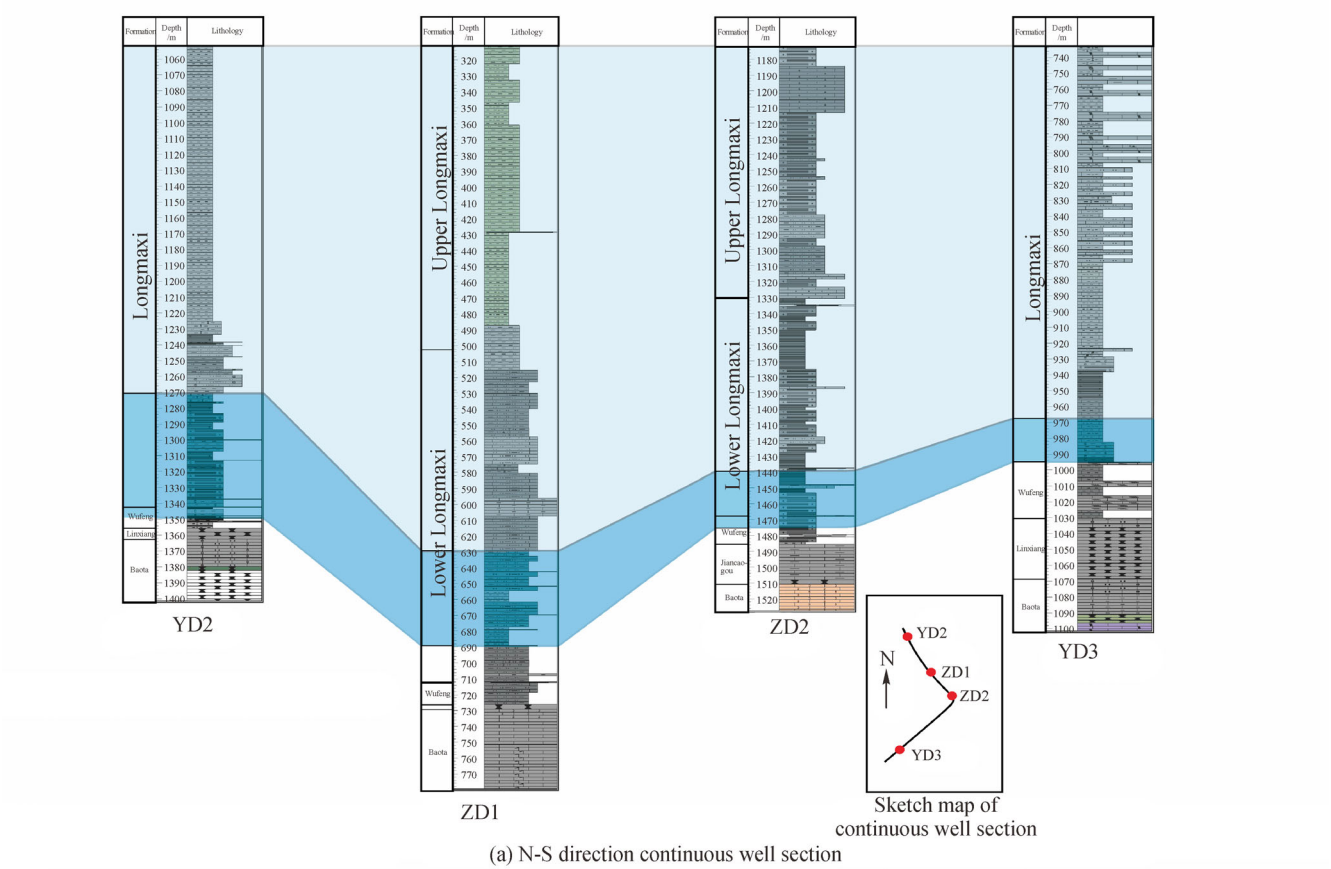

(a) N-S direction continuous well section

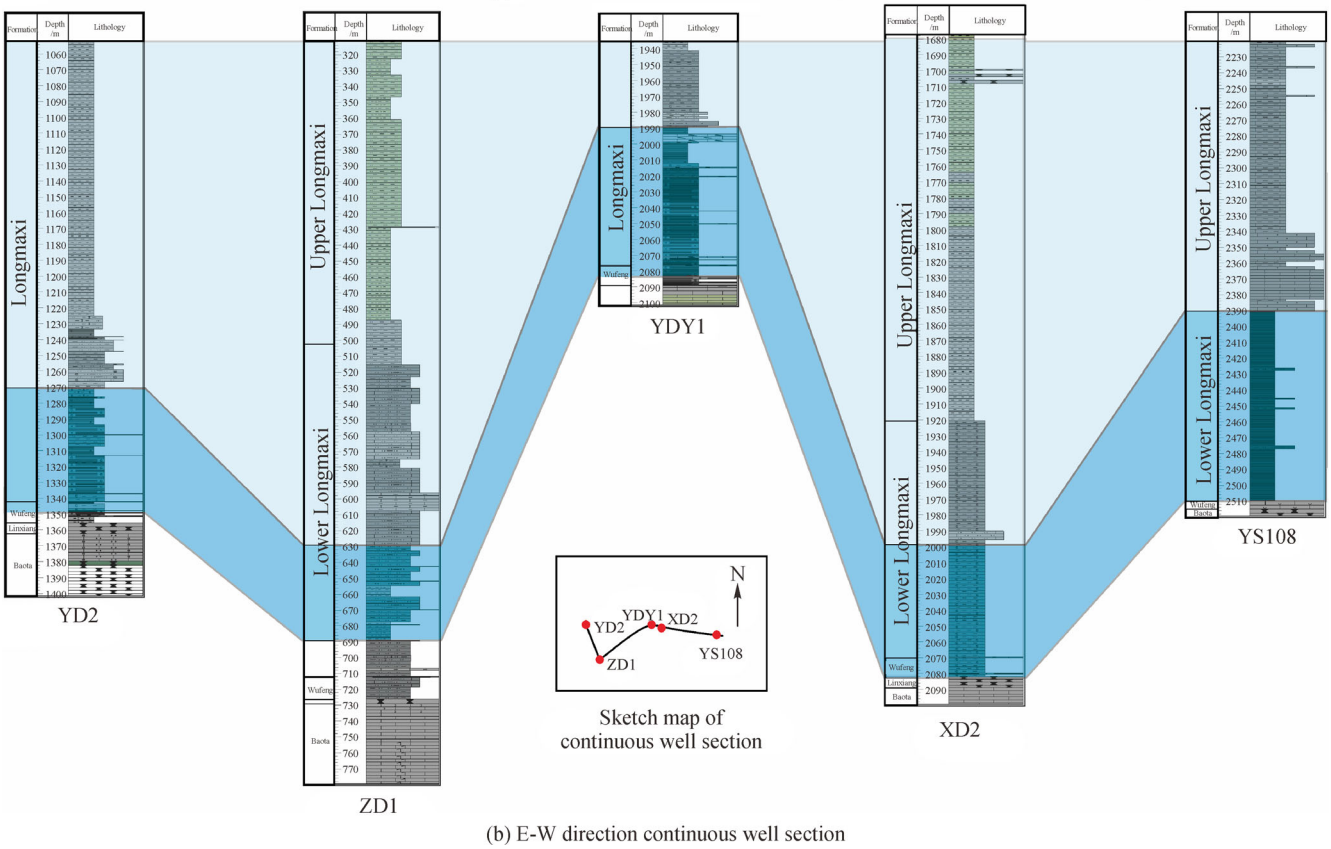

(b) E-W direction continuous well section

Fig. 8 Longmaxi Fm. Link well section in study area of (a) N-S direction continuous well section and (b) E-W direction continuous well section (Part of the data are from reference (Zhang, 2017)).

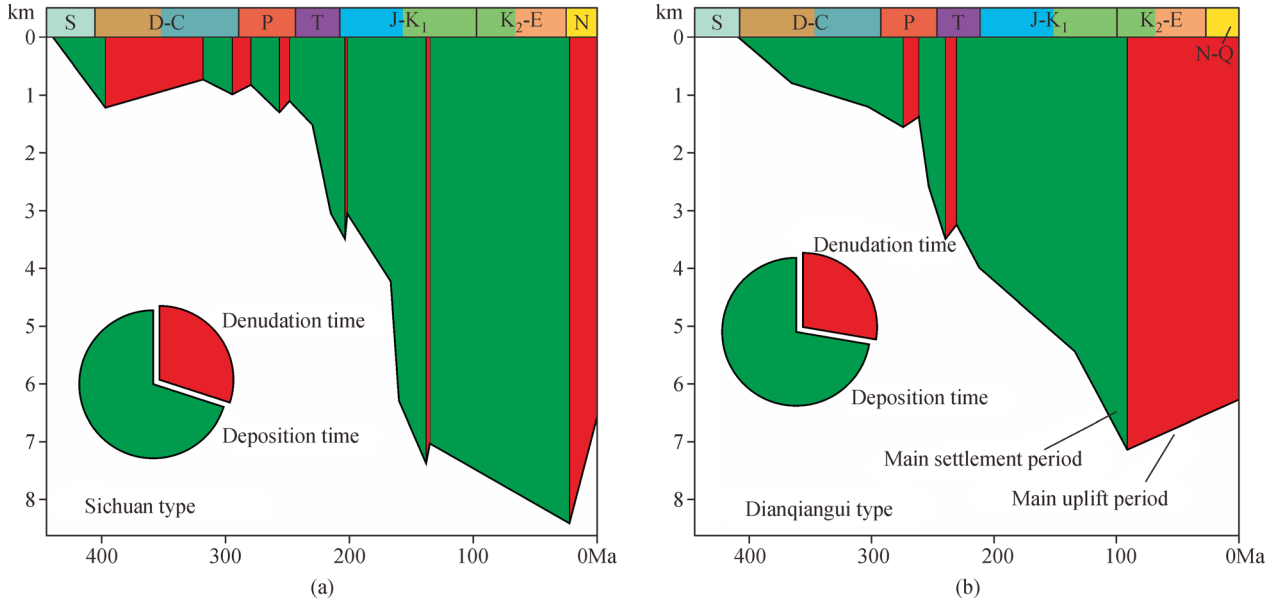

Fig. 9 Schematic diagram of burial history of Sichuan and Dianqiangui type in southern China (Modified from Wo et al. (2007b)). Pie chart shows the % of deposition and denudation time. (a) Sichuan type; (b) Dianqiangui type.

occurred in the late stage. Compared with Sichuan, the Dianqiangui type had a shorter subsidence period and a longer uplift period, and the uplift mostly occurred after the late Yanshan period. According to the results of the burial history restoration and structural locations, five typical wells in the area are divided into two types: syncline type (YD2, XD2, and ZD1) and anticline type (YD3 and ZD2), which belonged to the comprehensive Sichuan and Dianqiangui type (Fig. 9). They are characterized by continuous hydrocarbon generation, long sedimentation, and late accumulation of Sichuan type, and the uplift after the late Yanshanian period of Dianqiangui type. Huayingshan fault was first formed in the Lvliang movement of the Jinning period (Yang et al., 2010). The division between syncline and anticline type is based on the location of the well on the one hand. The syncline type was located in the Leibo Syncline in the northwest of Huayingshan fault, while the anticline type was located in the Daguan-Junlian anticline belt in the southeast of Huayingshan fault. On the other hand, it is divided according to the difference of the deposition-uplift process between the Hercynian and Indochina in the burial history curve. The anticline type can be clearly divided into two subsections during this period, while the syncline type is generally one deposition-uplift process.

5.3 Influence of tectonic movements for two types

Due to different structural positions, the controlling effect and manifestation of tectonic movements in different periods on the burial history of syncline and anticline types were also different. The result comparison is presented in Table 2.

5.3.1 Caledonian

The Caledonian movement in the study area was manifested as the changes of sea and land and originated from the horizontal extrusion of the Cathaysia Plate to Yangtze Plate in the northwest direction. Northeast Yunnan

Table 2 Comparison of similarities and differences between syncline and anticline type affected by tectonic movements

Period	Differences and reason	
	Syncline type	**Anticline type**
Caledonian	Unconformity surface between the formation of Silurian and Devonian	Unconformity surface between the formation of Devonian and Carboniferous
Hercynian	Dominated by extrusion stress, forming an unconformity contact surface	Shows the two subsidence uplifting process
Indosinian	Formation temperature rise rate was relatively slow and entered stage of medium maturity later	Formation accelerated heating rate and entered stage of medium maturity earlier
Yanshanian	Sedimentation-uplift rate, temperature rise rate, and maturity evolution process were similar, and the slight difference was mostly due to difference in maximum burial depth	
Himalayan		

is an episodic uplift area of the Caledonian movement, wherein the Yunan movement unconformity between the Cambrian and Ordovician, the Duyun movement unconformity between the Middle Ordovician and Silurian, and the Guangxi movement unconformity between the Silurian and Devonian were formed by the Caledonian movement. The Dianqiangui ancient land was formed after the Yunan movement in Cambrian and Duyun movement in Ordovician. Although transgression still occurred in the north, it did not cause a large-scale change. From the late Ordovician to Silurian, the earlier extensional plate boundary evolved into the collision plate boundary and the Dianqiangui ancient land finally evolved into the Dianqiangui basin at the end of Silurian (Zeng et al., 1994; Zhao and Ding, 1996; Mei et al., 2003). At the beginning of Devonian, the transgression from south to north caused the Devonian to deposit a set of transgression clastic rock series. The Ziyun movement in the transition period between the Devonian and Carboniferous strata led to the uplift of the crust, causing the Upper Devonian to regressively pinch-out from the south to north. During the Caledonian movement, regional transgression occurred, resulting in the deposition of Longmaxi Fm. The impact of Guangxi Movement on the study area weakened from the south to north. The anticline type in the south of the study area was affected by the Guangxi movement, forming unconformity between the Silurian and Devonian (Figs. 4(c) and 4(e)), while the syncline type in the north was generally unaffected by the Guangxi movement. The absence of Devonian and Carboniferous strata was primarily due to long-term effects of the Hercynian movement (Figs. 4(a), 4(b), and 4(d)). In the Caledonian period, the formation temperature slowly increased, and the maturity also gradually increased with the temperature. However, due to the shallow depth of strata in this period, the organic matter was in the immature stage (Fig. 5 and Fig. 6).

5.3.2 Hercynian

The Hercynian movement in the study area is primarily represented by a series of tectonic movements under the tectonic background of Guangxi movement at the end of Caledonian movement. All the Ziyun, Yunnan, Qiangui, Dongwu, and Emei tafrogeny movements took place in the continuous uplift stage of the Yangtze platform in the Hercynian period (Fig. 4). During the period of Dongwu movement, the syncline type was mainly impacted by the compressive stress, and the strata were uplifted and eroded, forming an unconformity contact surface. During the period of Caledonian movement and Hercynian movement, the anticline type generally demonstrated two subsidence uplift processes (Figs. 4(c) and 4(e)). In the Hercynian period, the strata of Longmaxi Fm. of synclinal and anticlinal types entered the stage of low maturity in succession except for the XD2 well. This is due to the difference in depth of strata because of different tectonic locations (Figs. 5(b) and 5(e)).

5.3.3 Indosinian

The Indosinian movement in the study area as a whole is characterized by a short uplift and denudation with a small amount of erosion, which had a little impact on burial history of the marine strata (Fig. 4). At this stage, the marine sedimentary history ended and the foreland basin sedimentary stage began. As a result of the Indosinian movement, the region was in a tension rifting environment, and the intracontinental rifting activities gradually intensified. At the end of the middle Permian, the Emei tafrogeny opened up the paleo Tethys Ocean and uplifted the thermal mantle column. Large scale basaltic magma erupted in the early stages of late Permian, resulting in the erosion discontinuity between the late Permian and middle Permian and the unconformity contact between the Maokou Fm. and overlying Longtan Fm. In the late Triassic, the Pacific plate subducted to the Yangtze block, paleo Tethys Ocean were closed, and Yangtze and Cathaysia plate were completely merged. Under the combined action of these factors, the passive continental margin evolution stage ended and the continental deposition stage began. During the Indochina movement, the depth of formation was rapidly deepened, and the heating rate of the anticline type formation accelerated (Fig. 6). The organic matter gradually entered the middle maturity stage, reaching the peak of oil production (Fig. 5), which was accompanied by the generation of pyrolysis gas. At this time, the formation was still in the initial accumulation stage. The syncline type had a slower heating rate than the anticline type; hence, its organic matter entered the middle-mature stage slightly later (Fig. 5).

5.3.4 Yanshanian

During the Yanshanian period, the Yangtze plate was dominated by the intraplate deformation, and the strata in the area continued to be deeply buried. The Yanshanian movement to the west of the Qiyueshan fault was weak and maintained subsidence and burial from the late Jurassic to the early Cretaceous. The stratigraphic contact relationship was mainly conformable contact or parallel unconformity. The strata under the unconformity of the Yanshan movement were well-preserved and basically not denuded (Fig. 4). By the middle of the early Cretaceous, the stratum burial depth reached its maximum value. At this time, the stratum temperature reached its maximum value, in general above 200°C (Fig. 6). Also, the organic matter entered the high-over-mature stage (Fig. 5), which was dominated by the generation of dry gas. Thereafter, the burial depth became shallower, the maturation process of

organic matter terminated, and the maturity no longer changed, while the geothermal decreased with the shallowness of burial depth. The uplifting process of the late Yanshanian movement eroded all the Upper Jurassic and Cretaceous strata, and the gas reservoir entered the adjustment period. As the XD2 well was located at the junction of two major faults, both the burial history and thermal evolution history were different from those of the other wells. Also, the sedimentary uplift rate, heat rate, and maturity evolution process of the anticline and syncline type were extremely similar in the Yanshanian period.

5.3.5 Himalayan

During the Cenozoic Himalayan tectonic period, the Indian plate squeezed northward while the Pacific plate subducted westward, causing the Upper Yangtze area to be subjected to two sets of stresses. Under the action of strong compressional stress, the strata continues to uplift until now. Owing to the Himalayan movement, the Triassic to Cretaceous strata in the area were completely eroded (Fig. 4). The uplift of the Yanshanian and Himalayan periods inhibited the hydrocarbon generation ability of the source rocks, and the secondary hydrocarbon generation capacity decreased with the shallowness of the burial depth until the end. Also, the difference in uplift was accompanied by the pressure difference, which was manifested in the regional differences. Thus, the existing gas in the formation migrate and accumulate in the favorable areas, and is destroyed and dissipated under unfavorable conditions. After the syncline and anticline types entered the Himalayan period, the evolution of maturity had already stopped. Also, the geothermal temperature also began to gradually decrease due to the uplift of the strata until it reached the current geothermal temperature. The syncline and anticline type had a small difference between the uplift curve and the geothermal curve in the Himalayan period. Overall, there was not much difference and the subtle differences were mostly caused by the differences in the maximum burial depth.

5.4 Shale gas accumulation process

According to the burial history, thermal history, and hydrocarbon generation history of five typical wells, the shale gas accumulation process of Longmaxi Fm. in the Northeast Yunnan can be divided into four stages (Fig. 10). First stage is the “source-reservoir-cap” sedimentary period. Affected by the Caledonian movement, widespread transgression occurred and dark mud shale of Longmaxi Fm. was deposited in the area. The burial depth continued to increase but the organic matter had not entered the mature stage. Second stage is the initial stage of the hydrocarbon accumulation. Different structural parts were impacted by varied tectonic movements, resulting in different burial history, which can be divided into anticline

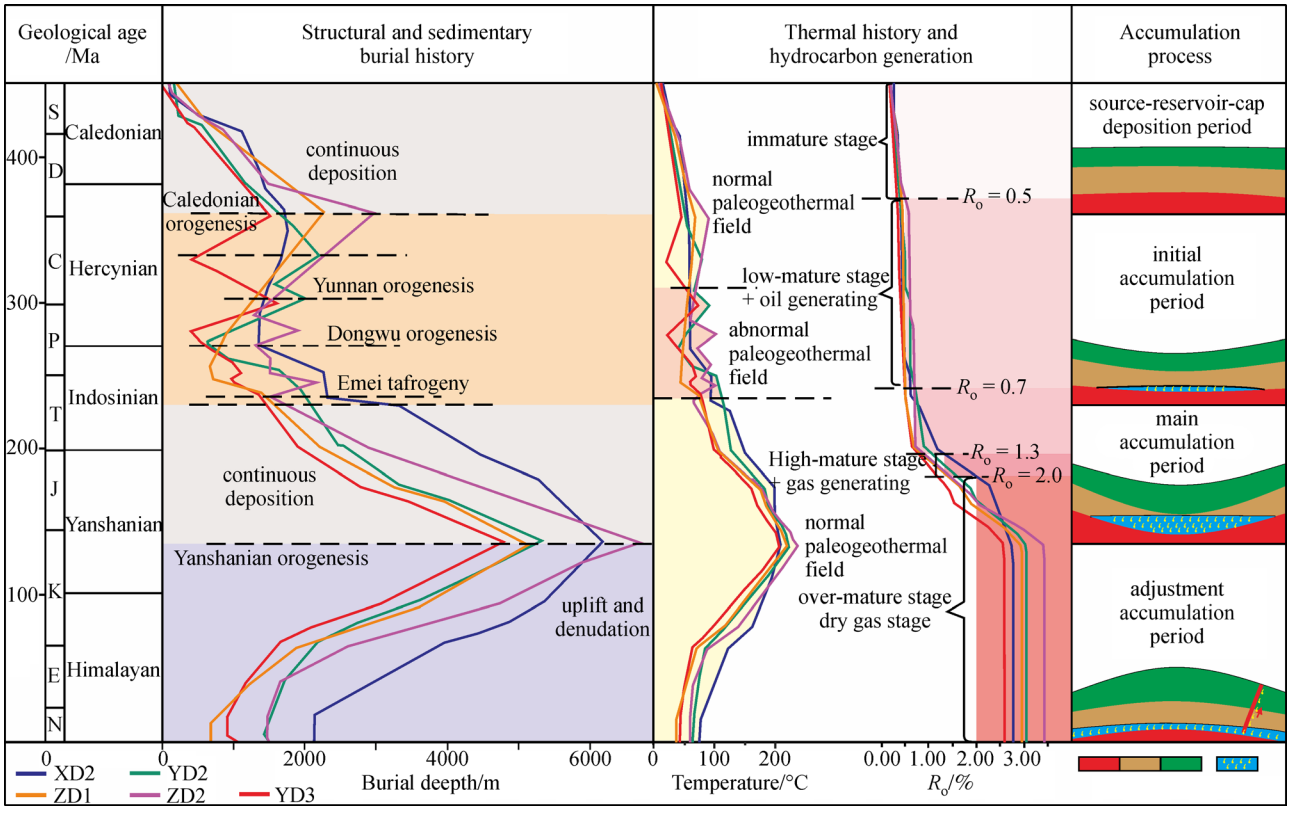

Fig. 10 Division of accumulation period.

and syncline type. In the initial stage of the hydrocarbon accumulation, the geothermal field was in a state of thermal anomaly due to the upwelling of thermal mantle plume. The Longmaxi Fm. generally entered the low mature stage, organic matter began to generate oil, which was accompanied by the biogenic gas. Third stage is the main accumulation period, during which the Indosinian and Yanshanian movements rapidly increased the depth of the stratum, geothermal temperature increased, organic matter maturated rapidly, and several hydrocarbon gases were generated in this period. Fourth stage is the adjustment of the accumulation period, which was mainly controlled by the late Yanshanian and Himalayan orogenic movements. Owing to the uplifting, the formation pressure was reduced, resulting in the fluid migration and rebalancing. The upper overburden of the Longmaxi Fm. was weakened due to the denustrations caused by the Yanshan and Himalayan movement, which may have damaged the gas reservoir cover and led to gas leakage, and even, lose the commercial value. Therefore, the thickness of the current Triassic and its overlying strata had a critical influence on the shale gas preservation of Longmaxi Fm.

The period from late Yanshanian period to late Himalayan period was a key duration for the formation of shale gas reservoir in Longmaxi Fm. and also for the structural transformation of the shale gas reservoir. The tectonic uplifting during this period may have led to the fault cutting of reservoirs, cessation of hydrocarbon generation process, destroying pressure system, and changing sealing preservation conditions etc. Therefore, later the tectonic uplift and denudation start, more favorable was the shale gas preservation process. Notably, due to an uplift between the Carboniferous and Triassic strata, it is necessary to consider the dissipation issue after initial hydrocarbon generation. During the first uplift, the shale of Longmaxi Fm. was in the low maturity, gas production was small, and uplift lasted for a short time. After uplift, it rapidly recovered to the continuous deep burial process. Therefore, the effect of this uplift on the shale gas formation was essentially whether the source rock was denuded and whether the material basis of gas generation was affected. Also, the uplift may have led to the development of pore fracture system, improve reservoir characteristics, and provide better storage conditions for the subsequent secondary hydrocarbons. Under the action of Yanshanian movement and Himalayan orogeny, the western area of Qiyueshan fault mostly formed barrier type fold belt. After undergoing structural deformation, it presented a structural combination of narrow anticlines and wide synclines. The overall deformation was relatively weak and the regional strata had good vertical and horizontal continuity. Therefore, the current thickness of overlying strata in the Longmaxi Fm. largely determined the preservation conditions of gas reservoirs. Also, during the evolution of geological history, the study area was mostly in a state of compression and the developed faults were mostly reverse faults. The fault zone was closed, fault sealing was good, and shale gas mainly migrated along the bed. Therefore, the transient uplift after the initial hydrocarbon generation had a relatively weak impact on the formation of gas reservoirs, and the vital controlling factors of shale gas accumulation in this area were the thickness of source rock, cap layer, and fault sealing property.

5.5 Guiding significance for shale gas exploration

The uplift and denudation processes lead to low pressure, which provides power for the oil and gas migration and accumulation. Uplifting and denudation led to relief and rebound of the formed reservoir pressure, which can provide more storage space for the hydrocarbon accumulation. The differential uplift of the strata may result in the faults or decrease the positive pressure of the fault plane, causing a weakening of the vertical closure. The capillary ability of the caprock is enhanced and the sealing ability of the pressure and hydrocarbon concentration are weakened due to the formation of uplift. The uplift rate of Longmaxi Fm. in the study area from the late Yanshanian period up till now ranges from 27 m/Ma to 38 m/Ma (29.4 m/Ma for XD2, 27.9 m/Ma for YD2, 27.5 m/Ma for YD3, 33.1 m/Ma for ZD1, and 28.2 m/Ma for ZD2). The lift rate is calculated by dividing the lift height by the lift time. The uplift rate demonstrated a negative correlation with the distance between each well and Huayingshan fault. The last uplift of each well in the area can generally be classified in three sections. The first section is after the Yanshanian period and before the Himalayan period. The second section is the early Himalayan movement, and therein, the uplift curve was steepest, indicating that the uplift rate was fastest during this period. The uplift rate of the third section was significantly lower than those of the previous two sections, suggesting that the tectonic movement had begun to stabilize at this time. Lower the rate of uplift formation, more was the time left for the previously balanced gas reservoirs to adjust. With the relief and rebound of the formation pressure, the reservoir performance was improved, which was more favorable for the integrity of the shale gas reservoir. Conversely, the faster the uplift rate is, the faster the gas reservoir balance is destroyed. The adjustment time is limited, and the overpressured gas reservoir inevitably breaks through the cap layer or escape along the bed, which is not conducive for the preservation of gas reservoir. According to the differences in the uplift curves of five typical wells, the uplift rate of the XD2 well was lowest during the first lifting process, which was most conducive for the gas reservoir adjustment. While the ZD2 well had highest uplift rate, which was most unfavorable for the preservation of gas reservoir. Since then, the uplift rate of each well increased, but after entering the third stage of uplift, the uplift rate of XD2 well slowed down first and maintained a

stable uplift rate for a long duration. This phenomenon provided sufficient time for the balance adjustment of gas reservoir. Finally, the wells successively stopped uplifting, forming the current state of the gas reservoir preservation. Based on the thickness distribution of the target layer, classification of burial history types, analysis of thermal history and hydrocarbon generation history, and comparison results of uplift rates, the following structural styles are considered to be favorable for the shale gas preservation, i.e. the area with wide and gentle anticline, the area with undeveloped faults or good fault sealing property or the footwall of fault blocked by fault, and the area relatively far away from the outcrop area or stratum denudation area and with deep buried target layer. The main body of the Changning Gas Field is a large saddle-shaped structure in a broad and gentle syncline. Jiaoshiba is a diamond-shaped fault anticline in the Wanxian syncline controlled by two groups' faults of north-east and near-south-trending. The deformation of the main structure is relatively weak. The seepage mechanism and migration and accumulation process of the two are in line with the regular gas accumulation law, that is, the positive structure is conducive to the enrichment of natural gas (Wang et al., 2016; Chen et al., 2017a; Liu, 2017). The deposition and uplift history of the Longmaxi Fm. in the Changning and Jiaoshiba areas is similar to that of the five wells in the study area in geological history, but the rate of that deposition-uplift process in the Permian to Cretaceous is slower compared to that in the study area, and the uplift rate in the last uplift process in the Changning area is also relatively slow, while that in the Jiaoshiba area is similar to that in this area (Fig. 11). From the above analysis, it can be concluded that the Longmaxi Fm. in the study area is generally similar to the Longmaxi Fm. in Changning and Jiaoshiba areas in terms of burial history evolution, and the successful experience of Jiaoshiba and Changning areas can be referred to for the drilling site selection.

6 Conclusions

This study focuses on the burial history, thermal evolution history and accumulation process of the Longmaxi Fm. in the Northeast Yunnan. According to the structural position of each well, the burial history curve can be divided into the anticline and syncline types. The Caledonian to Hercynian was the normal geothermal period, Hercynian to Indosinian before and after the Emei tafrogeny movement was the abnormal geothermal period, and the Indosinian period till now, the geothermal temperature has been restored to normal geothermal. The period from Indosinian to Yanshanian is the main accumulation period. The strata experienced continuous deep burial from Indosinian to Yanshanian and the geothermal temperature reached highest in the late Yanshanian. The maturity of organic matter reached highest at this time, generating a huge amount of gas. The major preservation factors of the shale gas reservoir adjustment period are the thickness of source rock, uplift rate, cap thickness, and fault sealing property. In combination with the structural positions of

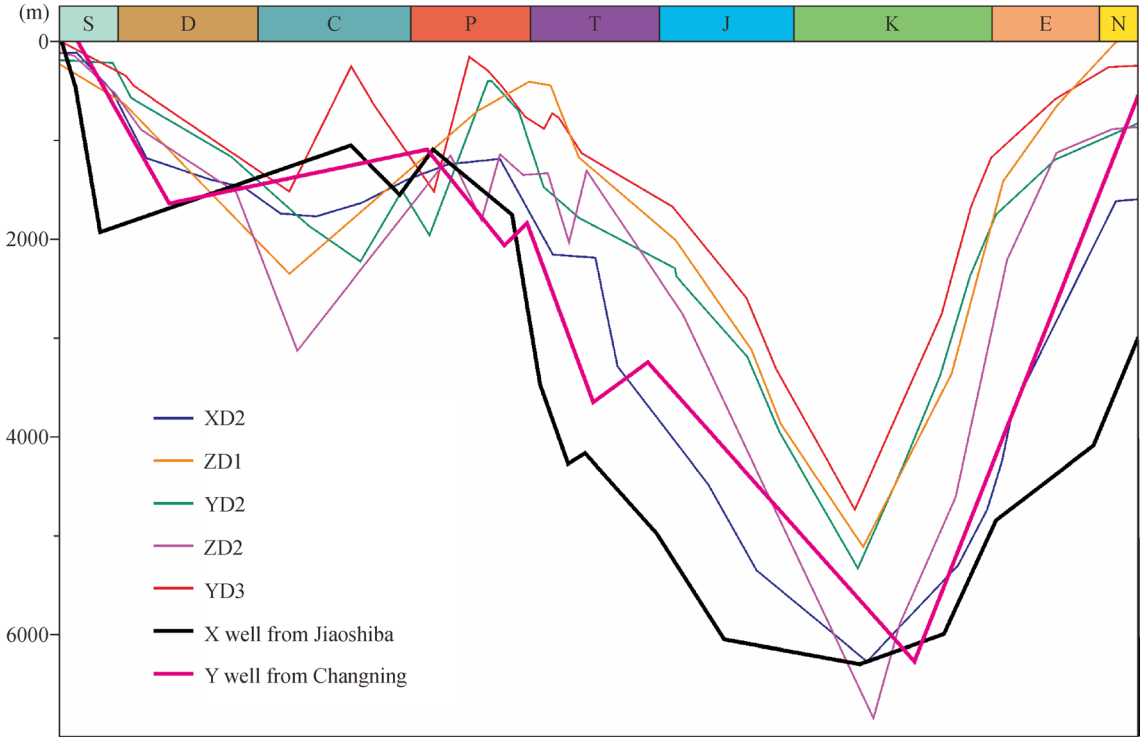

Fig. 11 Comparison of burial history of Longmaxi Fm. with typical drilled wells in Changning and Jiaoshiba areas.

typical drilling wells, the areas with wide and gentle anticline, far away from the denudation area, and deeply buried, with good fault sealing ability are priority structural locations for the shale gas exploration in northeast Yunnan.

Acknowledgements This study was supported by the National Natural Science Foundation of China (Grant Nos. 41772141 and 41802183).

References

Bai W H, Wang Q, Sun S S, Liang F, Zhang Q, Chang Y (2019). Geochemical characteristics and sedimentary environment of the Wufeng-Longmaxi shales: a case study from southwestern margin of the Sichuan basin. J China Univ Min Technol, 48: 1–14 (in Chinese)

Burnham A K, Sweeney J J (1989). A chemical kinetic model of vitrinite maturation and reflectance. Geochim Cosmochim Acta, 53(10): 2649–2657

Cao D Y, Nie J, Wang A M, Zhang S R, Zhang B (2018). Structural and thermal control of enrichment conditions of coal measure gases in Linxing block of eastern Ordos Basin. J China Coal Soc, 41: 14–23 (in Chinese)

Chen S B, Zhu Y M, Chen S, Han Y F, Fu C Q, Fu J H (2017a). Hydrocarbon generation and shale gas accumulation in the Longmaxi Formation, Southern Sichuan Basin, China. Mar Pet Geol, 86: 248–258

Chen S, Zhao W Z, Ouyang Y L (2017b). Comprehensive prediction of shale gas sweet spots based on geophysical properties: a case study of the Lower Silurian Longmaxi Fm. in Changning block, Sichuan Basin. Nat Gas Ind, 37(5): 20–30 (in Chinese)

Chen Z S, Xiao J X (1992). Characteristics of NNE-trending structure in the middle section of Huayingshan and its influence on mine development. Coal Geo China, 4: 1–8 (in Chinese)

English K L, Redfern J, Corcoran D V, English J M, Cherif R Y (2016). Constraining burial history and petroleum charge in exhumed basins: new insights from the Illizi Basin, Algeria. AAPG Bull, 100(04): 623–655

Fang R S (2000). A discussion about the Devonian stratigraphy of Yunnan. Yunnan Geo, 19: 62–90 (in Chinese)

Feng S, He J, Tian J J, Lu X Y, Yang B (2019). The characteristic and evolution of coal-forming swamp in Hanshuiquan district, Santanghu Coalfield, Xinjiang, NW China, during the Middle Jurassic: evidence from coal petrography, coal facies and sporopollen. Int J Coal Sci Technol, 6(1): 1–14

Gao R Q, Zhao Z Z, Jia C Z, Zhao Q B (2001). Oil and Gas Exploration in New Areas of China. Beijing: Petroleum Industry Press

Gottardi R, Adams L M, Borrok D, Teixeira B (2019). Hydrocarbon source rock characterization, burial history, and thermal maturity of the Steele, Niobrara and Mowry Formations at Teapot Dome, Wyoming. Mar Pet Geol, 100: 326–340

He Z L, Nie H K, Li S J, Luo J, Wang H, Zhang G R (2020). Differential enrichment of shale gas in upper Ordovician and lower Silurian controlled by the plate tectonics of the Middle-Upper Yangtze, south China. Mar Pet Geol, 118: 104357

Jiang N Y (1994). Paleogeography and Geochemical Environment of Permian in the lower Yangtze region. Beijing: Petroleum Industry Press

Jiang Y (2016). Study on Shale Gas Reservoir of Qiongzhusi Formation in Zhaotong-Qujing Area, Yunnan Province and Resource Prediction in Key Sections. Dissertation for Doctoral Degree. Kunming: Kunming University of Technology

Liu J (2008). Study on the Evolution of Paleogeothermal Field and Organic Matter Maturity History of Mesozoic and Paleozoic in Western Hubei and Eastern Chongqing. Dissertation for Doctoral Degree. Wuhan: China University of Geosciences

Liu Y K, Chang X (2003). Modeling of burial and subsidence history in Sichuan basin. Chin J Geophys, 46(2): 203–208

Liu P (2017) Structural Evolution and its Control on Accumulation of Shale Gas in Jiaoshiba area. Dissertation for Doctoral Degree. Xuzhou: China University of Mining Technology

Lu Q X, Ma Y S, Guo T L, Hu S B (2007). Thermal history recovery and hydrocarbon generation history of source rocks in Western Hubei and Eastern Chongqing. China. J Geol, 42: 189–198 (in Chinese)

Luo C, Wang L S, Shi X W, Zhang J, Wu W, Zhao S X, Zhang C L, Yang Y Q (2017). Biostratigraphy of Wufeng Formation Longmaxi Formation in well Ning 211 of Changning shale gas field. J Stratigr, 41: 142–152 (in Chinese)

Luo X, Vasseur G (1992). Contributions of compaction and aquathermal pressuring to geopressure and the influence of environmental conditions. AAPG Bull, 76: 1550–1559

Luo X R (1998). The concept, design and test of numerical model of sedimentary basin. Oil Gas Geol, 19: 196–204

Mei M X, Gao H J, Li D H, Meng Q F, Yi D H (2003). Devonian sequence stratigraphy and relative sea-level changes in Guizhou and Guangxi area, south China. Acta Sedimentol Sin, 21: 297–306 (in Chinese)

Morrow D W, Issler D R (1993). Calculation of vitrinite reflectance from thermal histories: a comparison of some methods. AAPG Bull, 77: 610–624

Nie H K, Li D H, Jiang T, Yan C N, Du W, Zhang G R (2020). Logging division method and significance of shale isochronal formation based on graptolite zone characteristics: a case study of Wufeng Longmaxi formation in Sichuan Basin and its periphery. Acta Petrol Sin, 41: 273–283 (in Chinese)

Pang Y, Guo X, Shi B, Zhang X, Cai L, Han Z, Chang X, Xiao G (2020). Hydrocarbon generation evaluation, burial history, and thermal maturity of the Lower Triassic–Silurian organic-rich sedimentary rocks in the central uplift of the South Yellow Sea Basin, East Asia. Energy Fuels, 34(4): 4565–4578

Pu B L, Dong D Z, Wang F Q, Wang Y M, Huang Z L (2020). The effect of sedimentary facies on Longmaxi shale gas in southern Sichuan Basin. Geol China, 47: 111–120 (in Chinese)

Qin Y, Wu J G, Zhang Z G, Yi T S, Yang Z B, Jin J, Zhang B (2020). Analysis of geological conditions for coalhed methane coproduction based on production characteristics in early stage of drainage. J China Coal Soc, 45: 241–257 (in Chinese)

Qiu D F, Li S J, Yuan Y S, Mao X P, Zhou Y, Sum D S (2015). Geological history simulation of the middle and upper Yangtze region and its petroleum geological significance. Pet Geol Recovery Effic, 22: 6–13 (in Chinese)

Qiu Z, Zou C N, Li X Z, Wang H Y, Dong D Z, Lu B, Zhou S W, Shi Z S, Feng Z Q, Zhang M Q (2018). Discussion on the contribution of

graptolite to organic enrichment and reservoir of gas shale: a case study of the Wufeng-Longmaxi formations in South China. Nat Gas Geosci, 29: 606–615 (in Chinese)

Straka P, Sýkorová I (2018). Coalification and coal alteration under mild thermal conditions. Int J Coal Sci Technol, 5(3): 358–373

Sweeney J J, Burnham A K (1990). Evaluation of a simple model of vitrinite reflectance based on chemical kinetics. AAPG Bull, 74: 1559–1570

Teng G E, Liu Y H, Xu W C, Chen J F (2004). The discussion on anoxic environments and its geochemical identifying indices. Acta Sedimentol Sin, 22: 365–372 (in Chinese)

Wang W, Zhou Z Y, Guo T L, Xu C H (2011). Early Cretaceous-paleocene Geothermal Gradients and Cenozoic Tectono-thermal History of Sichuan Basin. J Tongji Univ Nat Sci, 39: 606–613 (in Chinese)

Wang Y M, Huang J L, Wang S F, Dong D Z, Zhang C C, Guan Q Z (2016). Dissection of two calibrated areas of the Silurian Longmaxi Formation, Changning and Jiaoshiba, Sichuan Basin. Nat Gas Geosci, 27(3): 423–432

Waples D W (1980). Time and temperature in petroleum formation: application of Lopatin's method to petroleum exploration. AAPG Bull, 64: 916–926

Wo Y J, Xiao K H, Zhou Y, Yang Z Q (2006). Types of marine plays in southern China and exploration prospects. Oil Gas Geol, 27: 11–16 (in Chinese)

Wo Y J, Zhou Y, Xiao K H (2007a). The burial history and models for hydrocarbon generation and evolution in the marine strata in southern China. Sediment Geol Tethyan Geol, 27: 94–100 (in Chinese)

Wo Y J, Zhou Y, Xiao K H (2007b). Different regional characteristics of the petroleum accumulation conditions in the south of China. J Chengdu Univ Technol (Science and Technology Edition) 34:519–526. (in Chinese)

Wu CL, Zhang HN, Guo CX (1993). System view and methodology of basin simulation. J China Univ Geosci, 18: 741–747 (in Chinese)

Xiao C T, Li J M, Guo C X (1996). Reunderstanding of sedimentary environment of the Wufeng formation in mid-upper Yangtze area. ACTA Geol Sichuan, 16: 294–298 (in Chinese)

Xiao K H, Wo Y J, Zhou Y, Tian H Q (2006). Petroleum reservoiring characteristics and exploration direction in marine strata in southern China. Oil Gas Geol, 27: 316–325 (in Chinese)

Xu GR (1981). Stratigraphic correlation of Devonian in Yunnan province. Earth Sci, 2: 9–37 (in Chinese)

Yang R, Zhu S M, Xu C H, Zhou Z Y (2010). Fault sliding analysis and paleostress reconstruction of Huayingshan aults to East Sichuan basin. Inn Mong Petrochem Ind, 36: 97–100 (in Chinese)

Yang S, Hu W, Yao S, Wang X, He W, Wang Y, Zhu F, Sun F (2020). Constraints on the accumulation of organic matter in Upper Ordovician-lower Silurian black shales from the Lower Yangtze region, South China. Mar Pet Geol, 120: 104544

Ye S H, Jin C T, He Y X, Wan Z Q (1983). The Silurian stratigraphy of the Daguan area, Northeast Yunnan. BULL. Chengdu Inst Geol M R. Chinese Acad Geol Sci, 4: 119–140 (in Chinese)

Yuan Y S, Ma Y S, Hu S B, Guo T L, Fu X Y (2006). Present-day geothermal characteristics in South China. Chin J Geophys, 49(4): 1005–1014

Yuan Y S, Sun D S, Wo Y J, Zhou Y (2010). The relationship between burial history of marine strata and tectonic movements in Mid-Upper Yangtze area. Chin J Geol, 45: 707–717 (in Chinese)

Zamansani N, Rajabzadeh M A, Littke R, Zieger L, Baniasad A (2019). Organic petrology and geochemistry of Triassic and Jurassic coals of the Tabas Basin, Northeastern/Central Iran. Int J Coal Sci Technol, 6(3): 354–371

Zeng Y H, Zhang J Q, Liu W J (1994). Cambrian and Ordovician Lithofacies Paleogeography of Southern China. Beijing: Geological Publishing House

Zhang D, Yu Q, Lu J Z, Wang Z H, Zhao A K, Liu W, He J L, Lei Z H (2020a). Graptolite Biozonation of the Wufeng and Longmaxi Formations and Its Environmental Implications from the Xindi 2 Borehole in Yongshan-Daguan Area,NE Yunnan. Earth Sci (Paris), 45: 739–751 (in Chinese)

Zhang K, Song Y, Jiang S, Jiang Z, Jia C, Huang Y, Liu X, Wen M, Wang X, Li X, Wang P, Shan C, Liu T, Liu W, Xie X (2019). Shale gas accumulation mechanism in a syncline setting based on multiple geological factors: an example of southern Sichuan and the Xiuwu Basin in the Yangtze Region. Fuel, 241: 468–476

Zhang Q, Wang J, Yu Q, Wang X H, Zhao A Q, Zhang H Q, Wang Z H (2017). Black shales from the Longmaxi Formation in western Xikang-Yunnan ancient land: Geochemistry and geological implications. Sediment Geol Tethyan Geol, 37: 97–107 (in Chinese)

Zhang T S, Zhang Z C, Wu K Y (2016). Restoration of formation compaction and inversion of deposition rate in Dianqianbei exploration area. Lit Res, 28: 99–106

Zhang Z, Zhu X, Zhang R, Li Q, Shen M, Zhang J (2020b). To establish a sequence stratigraphy in lacustrine rift basin: a 3D seismic case study from paleogene Baxian Sag in Bohai Bay Basin, China. Mar Pet Geol, 120: 104505

Zhang Z C (2017). Evaluation of favorable shale gas areas of Longmaxi formation in Northern Yunnan and Guizhou. Dissertation for Doctoral Degree. Chengdu: Southwest Petroleum University

Zhao Y Y, Yan M C (1994). Geochemistry of Sediments in China's Shallow Sea. Beijing: Science Press

Zhao Z Q, Ding Q X (1996). Regional Stratigraphy in South Central Region. Wuhan: China University of Geosciences Press

Zhou B G, Wang Z Z, Ji P L, Jiang X S, Chen W Y (2018). Characteristics and sedimentary environments of the quartz sandstones in the Middle Devonian Suotoushan Formation in northeastern Yunnan. Sediment Geol Tethyan Geol, 38: 25–31 (in Chinese)

Zhu Y M, Zhou X G, Hu L (2014). Structural control of Taiyuan Formation shale gas reservoiring in southern Qinshui Basin. Coal Geol China, 26: 34–38 (in Chinese)